Conjugate Heat Transfer Simulations for a Film Cooled Nozzle Guide Vane of a High-efficiency, Industrial Gas Turbine

Karsten Kusterer, Jens Dickhoff, René Braun, Ryozo Tanaka, Tomoki Taniguchi, Dieter Bohn

Conjugate Heat Transfer Simulations for a Film Cooled Nozzle Guide Vane of a High-efficiency, Industrial Gas Turbine

Karsten Kusterer[1], Jens Dickhoff[1]*, René J. Braun[1], Ryozo Tanaka[2], Tomoki Taniguchi[2], Dieter Bohn[3]

ISROMAC 2016

International Symposium on Transport Phenomena and Dynamics of Rotating Machinery

Hawaii, Honolulu

April 10-15, 2016

Abstract

Great efforts are still put into the design process of advanced film-cooling configurations. In particular, the vanes and blades of turbine front stages have to be cooled extensively for a safe operation. The conjugate heat transfer (CHT) calculation technique is used for the three-dimensional thermal load prediction of an extensively cooled 1st nozzle test vane installed in a highest-efficient industrial gas turbine. With the CHT approach it is possible to take the interaction of internal flows, external flow, and heat transfer into account without estimation of heat transfer coefficients. The utilized numerical model contains all geometrical features (e.g. pin-fins, ribs, impingement sheets etc.) of the real test vane without simplifications. The comparison with thermal index paint measurements inside the test engine shows that a qualitatively and quantitatively good agreement between the CHT and the measurements results can be found. A consideration of advanced-shaped film cooling holes at the vane platforms also offers high potential to further reduce the material temperatures and decrease thermal stresses by lowering of platform temperatures and homogenization of the temperature distribution

Keywords

Gas Turbine — Conjugate Heat Transfer — Film Cooling — Thermal Index Paint Measurement

[1]*B&B-AGEMA GmbH, Aachen, Germany*

[2]*Kawasaki Heavy Industries LTD., Akashi, Japan*

[3]*RWTH Aachen University, Aachen, Germany*

***Corresponding author**: dickhoff@bub-agema.de

INTRODUCTION

In order to achieve high process efficiencies for the economic operation of stationary gas turbines and aero engines, extremely high turbine inlet temperatures at adjusted pressure ratios are applied. However, the allowable hot gas temperature is limited by the material temperature of the hot gas path components, in particular the vanes and blades of the turbine. Intensive cooling is required to guarantee an economically acceptable life span of the components (e.g. combustor walls, turbine vanes and blades, disks, etc.) that are in contact with the hot gas.

The initial design process of the cooled vanes and blades still depends on fast design procedures for the temperature field determination in the blade sections based on 1D and 2D calculation models for the internal flow path (1D network model) and the external flow of hot gas around the airfoil (2D boundary-layer code or 2D RANS calculation) coupled to a solid body heat conduction code by application of heat transfer correlations. However, the Conjugate Heat Transfer method for fully coupled three-dimensional flow field, heat transfer and heat conduction achieved more and more attention in the design process for modern gas turbines. With regard to the inter-relations between the external fluid flow, the internal fluid flow and the heat conduction, it is obvious that a coupled calculation can lead to a higher accuracy in thermal load predictions during the design process. Among others [1, 2], Bohn et al. [3 – 5] has developed a coupling approach at the Institute of Steam and Gas Turbines (IDG), RWTH Aachen University, which takes these considerations into account. It follows a homogeneous coupling procedure for the Conjugate Heat Transfer (CHT) calculations to be applied for thermal load prediction of cooled components in gas turbines. The method involves the direct coupling of the fluid flow and the solid body using the same discretization and numerical principle for both zones. This makes it possible to have an interpolation-free crossing of the heat fluxes between the neighboring cell faces. The detailed description of the conjugate calculation technique and its validation is provided by Bohn et al. in [6]. Today, the conjugate heat transfer procedure as explained above already became a standard application option in almost all modern commercial Computational Fluid Dynamics (CFD) tools. Furthermore, the CHT simulations of the cooled vanes and blades represent a state-of-the-art technology and an important step in the design process for the modern gas turbines. Depending on the kind of applied grid structures, such models today may include more than 60 million cells enabling the designers to take more and more geometric details into account within the simulation models.

Due to an application of the technology, it is possible to detect deficiencies of the cooling design process in an early stage. The deficits are caused by complex three-dimensional flow phenomena and uncertainties of applied heat transfer conditions. Their impacts cannot be considered by the simpler design approaches. The improved design based on the CHT technology contributes to the advanced design of the hot gas components by reducing the cooling air amount required to fulfil the cooling task and, as a result, it also contributes to the increase in thermal efficiency of the gas turbine cycle. Therefore, modern industrial gas turbines can achieve thermal cycle efficiencies above 40%. The recently developed Kawasaki L30A 30MWel gas turbine can be given as one example, claiming for the presently highest efficiency in its

class [7].
In the present study an extensively cooled state-the-art 1st stage nozzle guide vane is investigated. The vane has been analyzed based on the CHT technology under boundary conditions as to be expected in the gas turbine engine, i.e. realistic high temperature combustion gas flow. All details of the internal cooling structure (cooling chambers, impingement cooling, pin fins, ribs etc.) have been modelled without simplifications.
Furthermore, the test configuration has been implemented into a test engine at the Kawasaki Akashi plant and operated under a typical load condition of the gas turbine. Thermal Index Paint (TIP) measurements have been carried out and allowed the determination of the thermal load distribution – qualitatively as well as quantitatively.
Within the following sections, the numerical and experimental results are compared. Furthermore, the potential to improve the external vane cooling by application of advanced-shaped film cooling holes (NEKOMIMI-shaped configurations [8]) is presented. Besides others, the NEKOMIMI-shaped film cooling holes have shown the potential, to establishing anti-vortex film cooling structures and improve the film cooling effectiveness with respect to cylindrical but also to conventional laidback fan-shaped film cooling configurations.

1. INVESTIGATED GEOMETRY

1.1 Test Nozzle Guide Vane

The test vane investigated within the present paper represents a state-of-the-art nozzle guide vane for industrial gas turbines. It includes an internal convective cooling scheme with impingement cooling for further enhancement of the heat transfer on the internal walls. Numerous geometric features like ribs and pin fins also contribute to the advanced design for enhanced internal heat transfer.

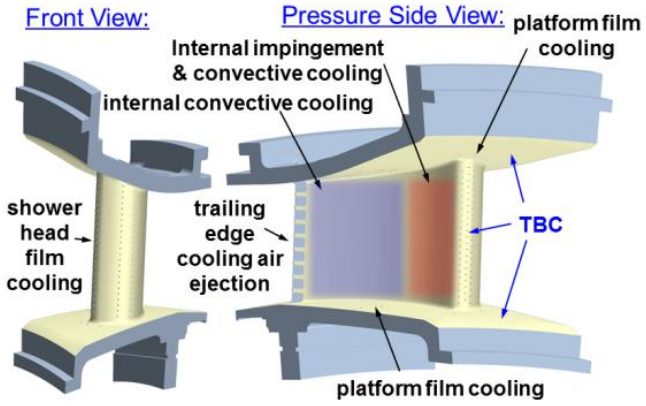

Figure 1. Solid body of the test nozzle guide vane with thermal barrier coating (TBC)

The leading edge of the vane is extensively film cooled by a showerhead cooling design consisting of several rows of inclined cooling holes. Additional film cooling is established along the suction side. A trailing edge injection of cooling air is provided through modern type cutback slots.

1.2 Advanced-Shaped Film Cooling Holes

Besides the improvement of every single gas turbine component, the efficient cooling of the hot gas path components is a major measure in order to reach a high efficiency of the gas turbine cycle. Film cooling is widely used for vanes and blades of turbine front stages in gas turbines in order to reduce material temperatures as far as necessary to ensure an acceptable life span of the components. As the cooling fluid is extracted from the compressor on high pressure levels, the reduction of the amount of cooling fluid for the cooling task leads to increased thermal efficiencies of the gas turbine.
Furthermore, film cooling leads to mixture losses and a reduced temperature of the hot combustion gas flow. Improvements can be achieved by reducing the cooling fluid amount and by establishing a more homogenous distribution of the cooling fluid on the surface.
Today it is well-known that film cooling effectiveness degradation is caused by secondary flows inside the cooling jets, i.e. the Counter-Rotating Vortices (CRV) or also named kidney-vortices, which induce a jet lift-off. The cooling fluid injection through a hole leads to a 'Jet in Cross flow' situation. The vortices are generated due to the interaction between the coolant jet and the cross flow.
A large number of publications deal with the experimental visualization or numerical calculation of these vortices. The publications of Bergeles et al. [9], Leylek and Zerkle [10], and Walters and Leylek [11] are mentioned as examples.
In order to establish anti-counter rotating vortices (ACRV) as major secondary flow phenomenon and enhance the film cooling effectiveness, Kusterer et al. [12] have introduced the Double-Jet Film Cooling (DJFC) technology. It utilizes the interaction between two separate inclined injection holes and the main flow. In 2011 Kusterer et al. presented a novel film cooling hole design derived from the DJFC-Concept – the patented NEKOMIMI technology (Japanese for "cat ears"), which has been patented [13] (see Figure 2).

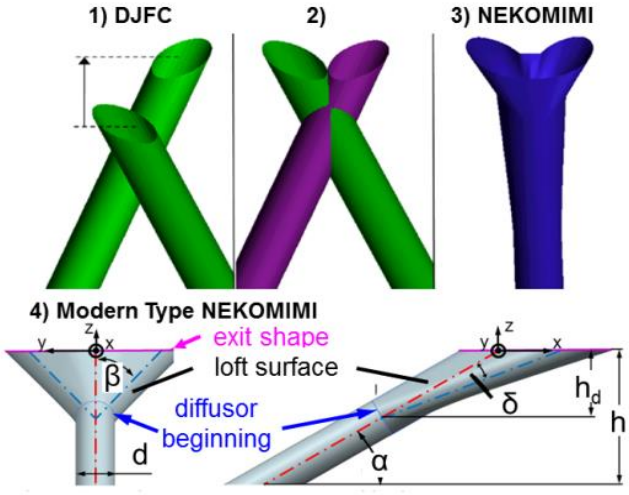

Figure 2. NEKOMIMI design concept

Like for conventional shaped film cooling holes, the diffusor part of the NEKOMIMI is intended to reduce the local

momentum flux ratio at the hole exit and the penetration of the coolant into the main flow. Simultaneously, ACRV can be established and their intensity adjusted in order to keep the mixing between hot gas and coolant low. The technology has shown potential to break the limits of conventional shaped film cooling holes in terms of the overall film cooling effectiveness.

2. EXPERIMENTAL MEASURMENT

In order to evaluate the surface temperatures of the test vane, Thermal Index Paint (TIP) measurements have been conducted. Today, TIP measurements are common practice for the investigation of the thermal load of gas turbine parts, which are exposed to high temperatures. The technology is based on the thermal activation of chemical reactions between metal elements and special pigments (mineral compounds) [14]. Metallic elements are provided by the test object itself (e.g. the nozzle vane body), while the pigments are part of the paint (mixture of solvents, binding agents and mineral fillers). By exposing the painted surfaces to high temperatures, the chemical reaction between metal and pigments changes the light reflection spectra. Thus, the human eye perceives a color change, which can be translated back to the local surface temperature of the test object. The reaction itself is irreversible, which means, that the resulting temperature distribution obtained from a TIP measurement represents only a composition of local peak temperatures occurred during the test run. This should be kept in mind while analyzing the measurement results. It also becomes clear, that it is of high importance to ensure constant boundary conditions during the test run without fluctuations. The technology allows an optical assessment of the resulting color of the tested gas turbine components offline only, after dismantling of the machine.

For the present TIP measurements a multicolor TIP has been applied to the nozzle vane surfaces. The typical layer thickness of such coatings is approximately 40µm [14]. Thus, the interference with the thermal behavior of the test object as well as the impact to the surrounding flow is minor.

The TIP measurement has been conducted on the gas turbine test rig at Kawasaki Akashi Plant, Japan (see Figure 3). More information about the test procedure, accuracy and calibration are given in [15])

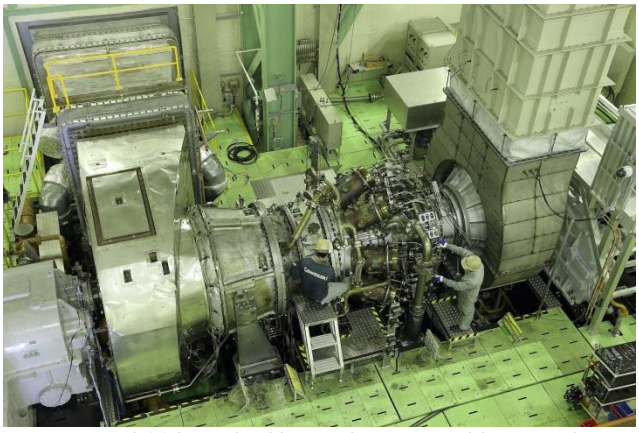

Figure 3. L30A on the Heavy duty gas turbine test rig at Kawasaki Akashi Plant, Japan

3. NUMERICAL METHOD

The CHT calculations have been carried out with the commercial CFD tool Star-CCM+ and the following calculation procedure and physical settings:

- three dimensional
- steady
- turbulent
- multi-component gas
- non-reacting
- ideal gas

The solver, calculation setup, procedure and mesh-settings have been benchmarked on basis of the well-known MARK II test case in 2012 [16]. Conjugate heat transfer calculations of the internally cooled blade, have been performed with Star-CCM+ as well as with the in-house code CHTflow [4].

The fluid domain considers a two gas component model, which handles the hot combustion gas and pure cooling air fluid properties separately. The dynamic viscosity, specific heat and thermal conductivity of the hot combustion gas are considered as polynomial functions in dependency of the static gas temperature in order to represent the gas composition inside the test engine behind the can-combustors.

The corresponding gas properties of pure air are related to the static temperature and the static pressure. They are deposited in a user library and correspond to the REFPROP data (NIST Reference Fluid Thermodynamic and Transport Properties Database) [17].

The material properties used for the solid region of the test vane represents a modern, state-of-the-art superalloy. In the CHT simulation, the thermal behavior is modelled by temperature dependent polynomial functions for the specific heat capacity and the thermal conductivity.

The turbulence is considered based on RANS (Reynolds-Averaged Navier-Stokes) equations and the k-ω SST turbulence model. In order to capture the heat transfer also in regions with wall y+ values above one, an all y+ wall treatment has been utilized, which automatically selects an appropriate wall treatment depending on the local y+ value.

The profile as well as the inner and the outer platform of the vane are coated with a ceramic layer (see Figure 1). Such thermal barrier coatings (TBC) are distinguished by a very low thermal conductivity. By its application, it is intended to reduce the heat input to the substrate and reduce the thermal loading of the coated component. Within the numerical model, the TBC layer has been considered as contact resistance (CR [m²K/W]), applied to the corresponding solid-fluid interfaces:

$$CR = \frac{t}{\lambda} \qquad (1)$$

(t: thickness of the TBC layer [m]; λ: thermal conductivity of the TBC [W/m-K])

3.1 Computational Domain

The computational domain of the CHT calculation is illustrated in Figure 4. It consists of a solid (left) and a fluid region (right). Congruent surfaces are defined as in-place interface and allow modeling of the heat transfer. The solid region corresponds to the test vane geometry provided by KHI. Small geometrical

features of the solid body have been removed as they are not affecting the fluid flow and have minor effect to the thermal behavior of the vane body.

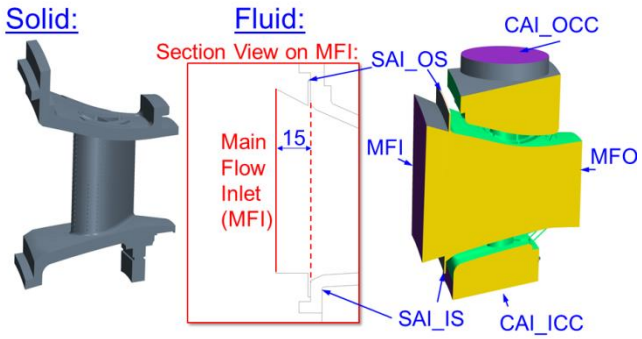

Figure 4. Computational Domain of the CHT simulation – solid and fluid body

The fluid region illustrated on the right hand side of Figure 4 consists of the following surfaces:

- one main flow inlet (MFI)
- two sealing air inlets (SAI) in-front of the inner (IS) and outer shroud (OS) platforms
- two cooling air inlets (CAI) – one at top (connected to the outer cooling chamber (OCC)) and one at the bottom of the domain (connected to the inner cooling air chamber (ICC))
- one main flow outlet (MFO)
- six periodic surfaces (main flow passage, inner cooling chamber and outer cooling chamber)
- adiabatic walls (grey)
- solid-fluid interfaces (light green)

The thermal load in the upstream region of the platforms is significantly influenced by the sealing air injection. Therefore, two sealing air inlets have been modelled in-front of the test vane.

The shape of the inner and outer cooling air chambers corresponds to the cavities inside the vane carrier.

3.2 Boundary Conditions

The CHT calculations have been performed with boundary conditions in accordance to operating conditions in the test engine.

At the main flow inlet of the fluid region, hot combustion gas is entering the domain. The velocity components have been prescribed to be boundary normal. A total pressure, a total temperature and a boundary normal flow direction have been prescribed. The end of the main flow passage is represented by the main flow outlet and modelled with a static pressure boundary.

The normalized radial profiles of total temperature at the main flow inlet and the static pressure at the main flow outlet are illustrated in Figure 5. The maximum total temperature is located at approx. 75% span. The absolute value drops by approx. 7% towards the inner and outer shroud platform. The static pressure profile at the main flow outlet is almost linear. The highest value is located close to the upper shroud. At the lower shroud the static pressure value is reduced to approx. $0.92*p_{st,max}$.

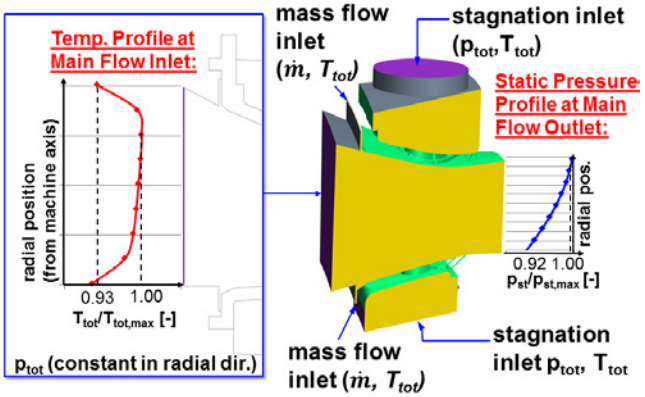

Figure 5. Boundary conditions applied to the fluid region of the test vane (principal).

For the solid region most of the surfaces are defined as fluid-solid interfaces. However, a few surfaces are in contact with the vane carrier or gasket ring structure when the vane is mounted into the gas turbine. An estimation of appropriate heat transfer coefficients for these surfaces is challenging. Furthermore the heat transfer at these surfaces is rather small. Therefore, the walls have been considered to be adiabatic, which corresponds to the assumption of an infinite contact resistance.

A heat transfer coefficient with corresponding reference temperature was defined at the blunt surface of the outer shroud (see Figure 6). The surface is located outside the fluid region of the computational domain but in contact with hot gas/sealing air in the real gas turbine. The HTC value has been derived with an estimation approach based on the VDI Heat Atlas [18], which is valid for fully turbulent flows in-between two flat plates (gap flow).

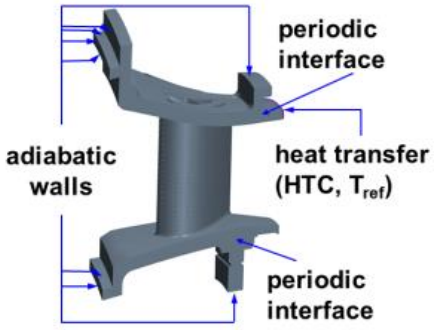

Figure 6. Boundary conditions applied to the solid body of the test vane.

3.3 Computational Mesh

The mesh of the computational domain (fluid and solid region) consists of unstructured polyhedral cells and has been generated in STARCCM+ 9.06. On the interfaces, prism layers are in use (on fluid side only) to keep the wall y+ values low and improve the heat transfer prediction accuracy.

Figure 7 gives an impression of the mesh. As visible the number and height of the prism layers have been adjusted to the current flow properties at the corresponding interfaces. Hence, on the outer airfoil interfaces, 20 prism layers with a

total thickness of 0.189mm were applied. The cell closest to the wall has a height of 3E-4mm. The stretching factor between the PL cells is 1.3.

On interfaces between the internal cooling devices, the hot gas side of the inner and outer shroud interfaces and inside the film cooling holes, 15 prism layers were meshed (height of the wall near cell: 8E-4mm). An application of PL to the cooling devices was not possible due to the high complexity of the structures. This has been accepted, since an all y+ treatment was used for all CHT simulations (see chapter 2) and due to the fact, that the heat transfer enhancement intended by application of ribs and pin-fins is mainly caused by their turbulence and vorticity augmentation. Thus, the heat transfer is also increased on the interspaces between the cooling devices – not only at the walls of the devices.

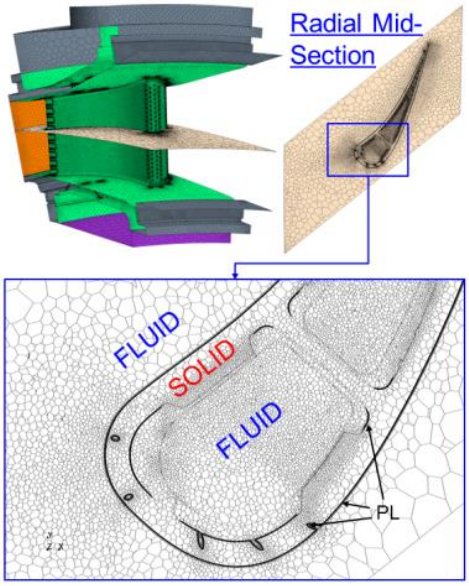

Figure 7. Computational mesh of the fluid and solid region – overview and mid-span section

Additional prism layers can be found on the interface between the outer cooling chamber and the outer shroud platform. Here, a minimum cell height of 6E-3mm is sufficient to achieve wall y+ values below or close to 1, due to the relatively low velocities within the cavity.

The resulting mesh consists of approximately 14 million cells.

On the external and internal surfaces in-between the cooling devices, y+ values below or close to one could be achieved.

4. RESULTS

4.1 Validation of the CHT calculation procedure

Within the following section, the CHT results are compared and analyzed to the experimentally obtained data.

A qualitative illustration of the surface temperature distribution on the pressure side of the vane is given in Figure 8. The TIP results (right hand side of the figure) show distinct temperature zones.

At approx. 50% chord length, the temperature increases over the complete profile span within a short axial distance. This is also represented in the CHT simulation (zone (2) in Figure 8). The high temperature gradient results from the different cooling schemes utilized inside the vane for the rear and front part. In the rear, a pin-fin array is placed, while the front part of the vane is cooled more intensively by impingement jets.

The TIP measurement furthermore shows relatively low temperatures in upstream regions of the upper and lower shroud platforms due to sealing air injections located in-front of the shrouds (zone (1) and (3)). This is in good agreement with the temperature distribution obtained from the CHT simulation.

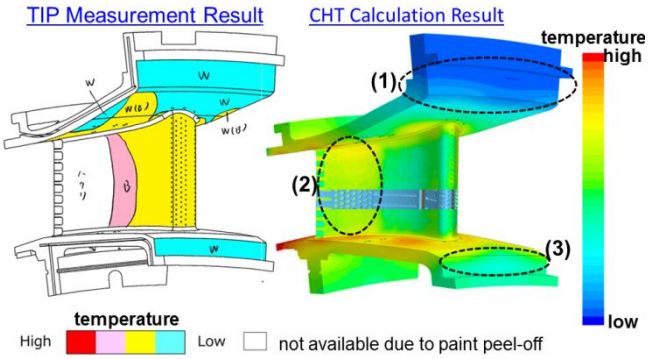

Figure 8. Surface temperature of the test vane – TIP measurement and CHT results

However, a zone with slightly increased surface temperatures (yellow) is located at the outer shroud platform towards the pressure side of the test vane, which is not captured by the CHT simulation. It can be presumed, that this is due to an inhomogeneous sealing air outflow in circumferential direction, but it might also be a result of the TIP measurement technique. As stated above, the color change of the paint is irreversible. Thus, the locally measured temperature corresponds to the maximum temperature occurred during the complete test run. Zones with increased temperatures might have been exposed to significantly higher temperature for a relatively short time period. However, the temperature distribution of the CHT simulation represents a time averaged surface temperature at all positions.

A view on Figure 9 reveals that the discussed temperature increase around 50% chord is also represented on the suction side (see zone (2)), but according to the temperature distribution obtained from the CHT simulation, the magnitude of the temperature increase is noticeably smaller. Furthermore the TIP measurement result suggests that the temperatures are higher at the inner part of the profile.

Close to the trailing edge, measurement and calculation show small areas with increased temperatures, distributed over the profile span (zone (4)). The position is influenced by the cutback slot geometry on the pressure side of the vane. On the opposite side of the lands in-between the cutback slots, the solid temperatures are locally increased (see Figure 9). Positions, which can be cooled more intensively by the ejected coolant, reveal a reduced thermal load (between the locations with increased temperatures – opposite side of the cutback slots).

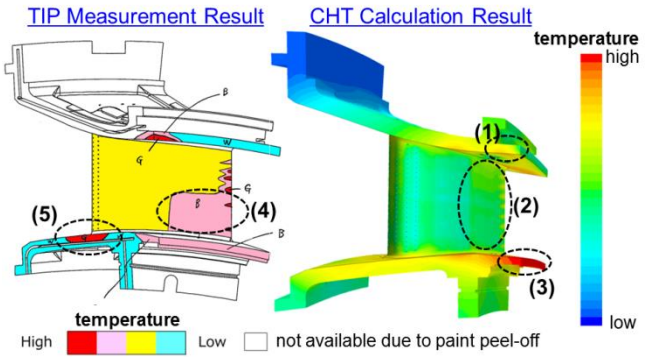

Figure 9. Surface temperature of the test vane – TIP measurement and CHT results

A detailed view on the surface temperature distribution on the outer shroud platform is illustrated in Figure 10. Generally, the numerically obtained temperature distribution is in good agreement with the measurement results, but it should be kept in mind, that the result of the TIP measurement represents an ensemble of local maximum peak temperatures, while the surface temperatures obtained from the CHT analysis represent averaged values under ideal conditions and without fluctuations. Local differences in terms of the surface temperature are consequently not avoidable.

Two relatively cold zones, one located behind the sealing air injection in-front of the platform (zone (1)) and one close to the pressure side of the vane (zone (2)) are visible for the CHT and the TIP approach. Furthermore, a region with moderate temperatures (colored yellow) starts from the leading edge of the vane and propagates towards the end of the platform. As presented by the CHT simulation result, the temperature gradually increases in axial direction. However, the rough division of the TIP measurement colorbar suggests a more rapid change of the temperatures close to the trailing edge of the platform, which easily leads to a misinterpretation. This is a good example, which shows how CHT and TIP results can complement each other in order to improve the design of gas turbine components exposed to high temperatures. The measurement serves as validation basis for the numerical results. And the CHT simulation allows a deeper insight into flow phenomena in order to increase the understanding for the obtained resulting temperature distribution on the part surfaces.

On the platform near the suction side (zones (4), (6) and (7)), the CHT simulation result shows regions with increased temperatures. The TIP measurement technique is not able to resolve those locally increased temperatures due to the small number of temperature levels available. Every color represents a relatively wide temperature range. Additionally, cooling air may have been escaped from the lateral gap between two neighboring nozzle vanes in the experimental measurement, which can cause a temperature reduction in zone (6) and (7). This sealing air is not modelled within the CHT simulation (flanks of the solid vane body are considered as periodic surfaces). Thus, zones (3) and (4) propagate towards the neighboring vane and build zones (7) and (6) respectively.

Zones (3) and (5) are reproduced by the measurement and the simulation result. Zone (5) is located at the very end of the outer shroud platform – downstream of the outer cooling chamber (OCC). An extensive cooling by the OCC is consequently not possible. Furthermore the bearing structure of the vane carrier is located above this part of the shroud platform when the nozzle vane is installed in the machine. Thus, the cooling effect by sealing air, which is injected behind the outer shroud platform, is small. However, on the blunt surface at the end of this platform, the sealing air is reducing the surface temperature. This is reproduced by the TIP measurement as well as by the CHT simulation result.

For zone (3), the CHT result shows, that the region with increased surface temperatures is rather small and the magnitude of the temperature is lower than obtained from the TIP measurement. This is more realistic than the rapid temperature change shown for the TIP result, in which the temperature is changing by two temperature steps from yellow to red (pink is not visible). A explanation reason is that the surface has been exposed to locally very high temperatures for a short time period, but it might also be a measurement or data acquirement failure.

Upstream of zone (3), a double jet film cooling pair is located, but the CHT results display that the downstream effect is too small to avoid a temperature increase on the outer shroud platform towards the profile trailing edge.

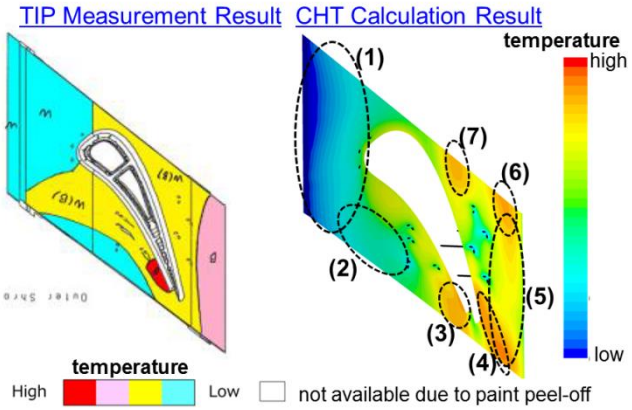

Figure 10. Surface temperature on the outer shroud platform of the test vane – TIP measurement (left) and CHT results (right)

For the inner shroud platform, the measurement results also show increased surface temperatures close to the profile, beginning at approx. 50% span. This is reproduced by the CHT simulation result as well (cf. zones (3) and (4)). Downstream of zone (4), the results obtained from calculation show a strong temperature reduction caused by the double jet film cooling arrangement. Small regions with considerably low temperatures, resulting from the generated cooling air film, could be reproduced with the TIP measurement technique as well (colored in blue).

Zone (1) is reproduced with both approaches, too. As discussed above, sealing air is injected in-front of the inner and outer shroud platforms resulting in a locally reduced surface temperature. For the CHT simulation, a coolant mass flow inlet has been modelled in-front of the vane. Over the circumference, a constant cooling air mass flow is injected in negative radial direction (fully homogenous mass flux dist. in circumferential direction). However, comparison between the

cold zones (1) obtained from the experiment and the calculation, with respect to their shape, suggests that the sealing air outflow in the real gas turbine is not fully homogenous or even fluctuating.
Zone (2) is not directly represented by the measurement results, due to the low number of temperature steps, but the yellow color indicates, that the sealing air injected in-front of the platforms is not capable of cooling this region that intensively. It is mixed out with hot combustion gas before reaching the position of zone (2).
Another region with increased temperatures is located at the downstream part of the inner shroud platform (zone (5)). As discussed for the outer shroud platform (zone (5) in Figure 10) the rear parts of the platforms cannot be cooled by the inner/outer cooling chambers. Furthermore, it is challenging to establish a high heat transfer on the surfaces, which are opposed to those in contact with the main flow passage, due to the position of the connected nozzle vane support structure (e.g. vane carrier).

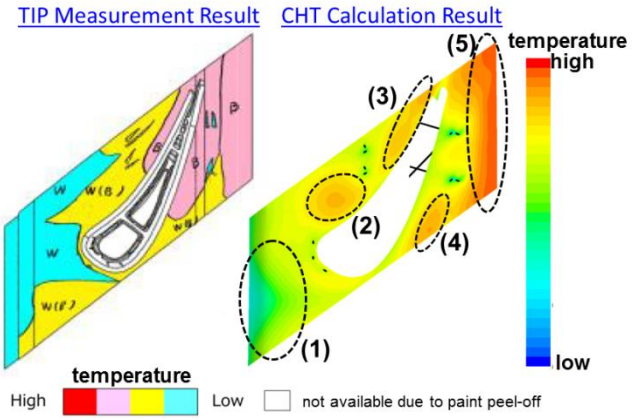

Figure 11. Surface temperature on the inner shroud platform of the test vane – TIP measurement (left) and CHT results (right)

4.2 Application of Advanced-Shaped Film Cooling Holes

On the platforms of the tested 1st nozzle guide vane, double jet film cooling (DJFC) holes have been utilized. This leads to a sufficient cooling with respect to the maximum allowable wall temperature on the platforms.
The DJFC technology has been invented with the intention to establish anti-counter rotating vortices (ACRV) and thus augment the film cooling effectiveness. As mentioned in section 1.2, this advanced film cooling technology consists of a pair of cylindrical cooling holes. The relative position and orientation between the two holes and the approach flow direction is a key parameter to establish the desired ACRV. Precise knowledge of the exact flow direction close to the platform surfaces is consequently essential but difficult to predict without modern measurement or calculation techniques.
In Figures 12 and 13 the platforms of the test vane are shown after 4900 operating hours (right and left hand side of the two figures). The thermal barrier coating has changed its color. It gives a qualitative indication of the temperature on the shroud platforms and therewith information about the flow directions close to the walls downstream of the DJFC holes.

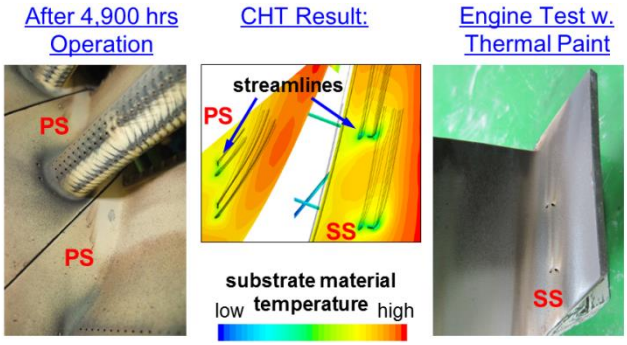

Figure 12. Inner shroud platform of the test vane after 4900 operating hours (right and left) and the CHT result (center) with streamlines starting inside the film cooling holes.

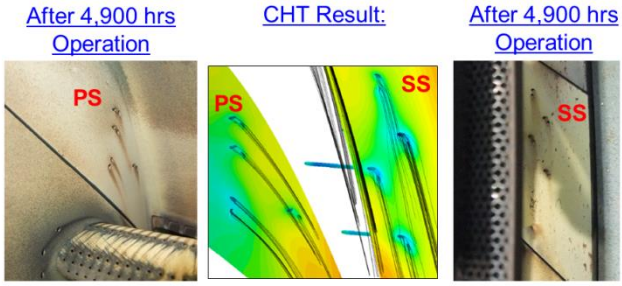

Figure 13. Outer shroud platform of the test vane after 4900 operating hours (left), of the thermal index paint measurement (right) and the CHT result (center) with streamlines starting inside the film cooling holes.

The CHT simulation results are illustrated in the center of Figures 12 and 13. Streamlines indicate the direction of the film cooling air ejected through the DJFC pairs.
A comparison between the TBC discoloration and the CHT results shows that the calculated flow directions are in very good agreement with the ones inside the real gas turbine. Additionally both results show potential for the improvement of the DJFC hole orientation. However, due to the complex supply situation (connection to the inner/outer cooling chamber), the possibilities for variation of the DJFC hole arrangement and orientation are limited.
To compensate this drawback of the DJFC technology, the NEKOMIMI-shaped film cooling holes have been invented. With one main supply hole, the transfer of the cooling air from the cooling chamber to the hot external surfaces of the gas turbine parts has been simplified significantly.
It should be noted, that the following numerical comparison between the double jet and the NEKOMIMI film cooling approach, has been carried out on the basis of slightly different boundary conditions with respect to the simulations presented in section 4.1 and 4.2. The two simulations carried out for the present section – one with DJFC and one with NEKOMIMI-shaped film cooling holes – correspond to another load state of the engine.
Figure 14 shows the mass fraction of the coolant inside the gas mixture on the inner and outer shroud platform. These values give an indication of the adiabatic film cooling

effectiveness on the walls. The local temperature of the fluid inside the cooling film is influenced by the thermal conduction inside the fluid, radiation and the mixing between hot combustion gas and cooling air. The latter leads to a changed coolant mass fraction and governs the fluid temperature – especially within the region close to the film cooling hole, where the mixing process is strong (cf. [20]).
Furthermore the footprints of the coolant mass fraction behind the film cooling holes give a good indication whether the NEKOMIMI is properly oriented or not (see Figure 14). Additionally, this result allows a comparison between the more theoretical studies on the NEKOMIMI technology based on the typical test case with ideal boundary conditions and on a flat surface without cross flows or pressure gradients on the test section (e.g. [8] or [19]).
The current setup consists of two NEKOMIMI types, which are visible on the inner and outer shroud platforms. The main difference is the lateral distance (regulated with the angle β; cf. Figure 2) between the ears and the laidback angle (δ; cf. Figure 2). A higher lateral distance leads to a wide film cooling footprint (configuration presented in the center of Figure 14). Thus, the film cooling air remains close to the wall and covers a relatively wide part of the hot shroud surface. Furthermore, a bimodal pattern is formed for this type of NEKOMIMI holes, which is desired, promotes the generation of ACRV and therewith further enhances the film cooling effectiveness. However, a high lateral distance between the NEKOMIMI ears lowers the robustness of the film cooling hole against compound angles between the NEKOMIMI orientation and the approach flow. Thus, the orientation becomes more challenging. Otherwise the coolant mass flow may be distributed uneven inside the diffusor part and the bimodal pattern cannot establish.

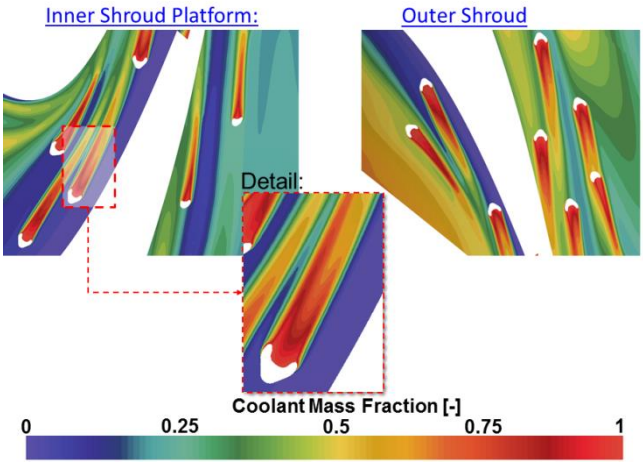

Figure 14. Coolant mass fraction on the inner and outer shroud platform

The NEKOMIMI-shapes with smaller lateral and streamwise propagation are more robust with regard of compound approach flow angles and perform better, when the orientation is not optimal due to restriction by the supply air situation or if the holes are located in regions with high static pressure gradients on the wall. The latter has an impact to the coolant mass flux distribution inside the diffusor of the shaped hole.

From these considerations it becomes clear, that the orientation and selection of adequate shaped film cooling holes for the application inside a gas turbine is challenging and requires profound knowledge about the technology.
Figure 15 shows the surface temperature on the outer shroud platform for the DJFC and the NEKOMIMI configuration. As shown in section 4.1, two zones with increased temperatures are located close to the trailing edge (zones (3) and (1)), which propagate towards the neighboring vane (zones (2) and (4)).

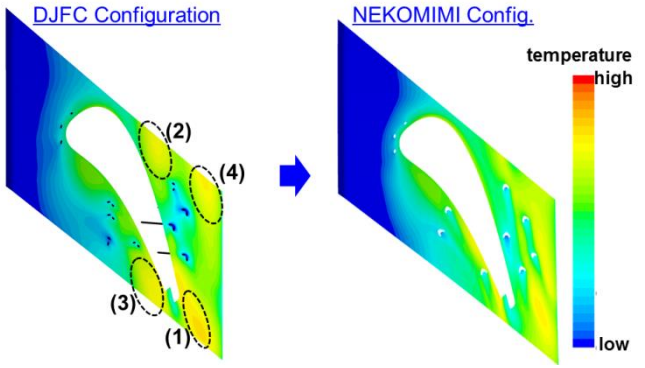

Figure 15. Surface temperature obtained for the outer shroud platform with the double jet film cooling (DJFC) and the NEKOMIMI design.

An improvement of the platform temperatures has been achieved by application of a NEKOMIMI hole close to zone (1), this region with increased temperatures could be avoided. Additionally, zone (3) has been weakened. The application of the shaped film cooling holes has led to a more homogenous temperature distribution on the complete pressure side of the outer shroud surface.
In the downstream part of zone (3), an additional NEKOMIMI hole has been placed. The established cooling film proceeds towards the neighboring vane platform. Besides the temperature reduction in zone (3), this also leads to a reduction of the thermal load in zone (2).
On the inner shroud platform (see Figure 16) the DJFC holes inside zone (4) lead to a significant reduction of the temperatures, but this also leads to increased temperature gradients due to the locally very restricted effect of the DJFC holes.

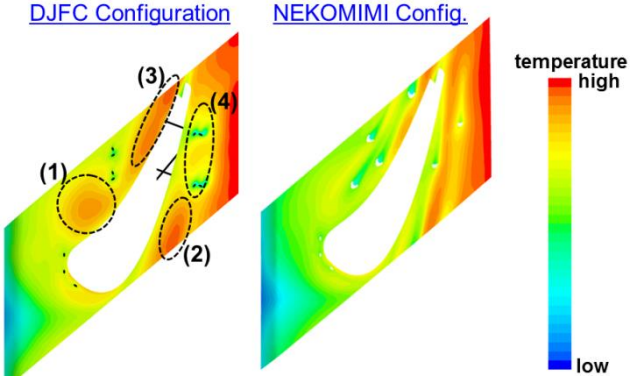

Figure 16. Surface temperature obtained for the inner shroud platform with the double jet film cooling (DJFC) and the NEKOMIMI design.

With the implementation of NEKOMIMI cooling holes, the temperature gradients could be reduced, but the maximum wall temperature is still on the same level as obtained for the DJFC configuration and located at the end of the platform. Due to the complex supply situation it is not possible to reposition the cooling hole exits towards higher axial positions to compensate the increased temperatures.
In total three additional NEKOMIMI film cooling holes have been added to the test vane with regard to the number of DJFC holes – two to the inner and one to the outer shroud platform. One film cooling hole has been removed. However, the total coolant consumption for platform cooling could be reduced by 27%, while the surface temperature distributions on the inner and outer shroud platform have been significantly improved.

5. CONCLUSION

The present paper discusses the calculation procedure and the accuracy of conjugate heat transfer calculations for a modern, extensively cooled 1st nozzle guide test vane in comparison to thermal index paint measurements.
In general, numerical results are in good agreement with the experimental test engine data in terms of the wall temperature distribution and the direction of the coolant propagation after ejection through double jet film cooling holes, which are located on the inner and outer shroud platform.
The paper furthermore shows how CHT simulations and TIP measurements can complement each other in order to obtain detailed information about the external and internal wall temperature distribution of gas turbine components exposed to high temperatures. The understanding of flow phenomena can be deepened and reasons for zones with increased temperatures can be figured out, which is essential in order to improve the design.
The application of the NEKOMIMI film cooling holes on the inner and outer shroud platforms is one example for a successful design improvement.

ACKNOWLEDGMENTS

The numerical simulations presented in this paper have been performed with the commercial software package STAR-CCM+ by CD-adapco. B&B-AGEMA and Kawasaki Heavy Industries would like to thank CD-adapco for their support

REFERENCES

[1] Li, H. J. and Kassab, A. J. 1994, „A Coupled FVM/BEM Approach to Conjugate Heat Transfer in Turbine Blades", AIAA-paper 94-1981, 1994

[2] Rigby, D. L. and Lepicovsky, J., "Conjugate Heat Transfer Analysis of Internally Cooled Configurations", ASME Paper 2001-GT-405.

[3] Bohn, D., Bonhoff, B., "Berechnung der Kühl- und Störwirkung eines filmgekühlten transsonisch durchströmten Turbinengitters mit diabaten Wänden", *VDI-Berichte 1109*:261 - 275, 1994.

[4] Bohn, D., Bonhoff, B., Schönenborn, H., "Combined Aerodynamic and Thermal Analysis of a High-pressure Turbine Nozzle Guide Vane", IGTC-108, Yokohama, Japan, 1995.

[5] Bohn, D., Bonhoff, B., Schönenborn, H., Wilhelmi, H., "Prediction of the Film-cooling Effectiveness in Gas Turbine Blades Using a Numerical Model for the Coupled Simulation of Fluid Flow and diabatic Walls", *ISABE 95-7105*:1150 - 1159, Melbourne, Australia, 1995.

[6] Bohn, D., Krüger, U. and Kusterer, K., "Conjugate Heat Transfer: An Advanced Computational Method for the Cooling Design of Modern Gas Turbine Blades and Vanes," in *Heat Transfer in Gas Turbines*:58-108, Sundén B and Faghri M (eds). WIT Press, Southampton, 2001.

[7] Tanaka, R., Koji, T., Ryu, M., Matsuoka, A. and Okuto, A., "Development of High Efficient 30 MW Class Gas Turbine: The Kawasaki L30A", ASME-paper GT2012-68668, Copenhagen, Denmark, 2012.

[8] Kusterer, K., Elyas, A., Sugimoto, T., Tanaka, R., Kazari, M., and Bohn, D., "The NEKOMIMI Cooling Technology: Cooling Holes with Ears for High-efficient Film Cooling", ASME-paper GT2011-45524, Vancouver, Canada, 2011.

[9] Bergeles, G., Gosman, A. D., and Launder, A. D., 1976, "The Prediction of Three-dimensional Discrete-hole Cooling Processes", *Journal of Heat Transfer*, 98, pp. 379-386.

[10] Leylek, J. H., and Zerkle, R. D. 1994, "Discrete-Jet Film Cooling: A Comparison of Computational results with Experiments", ASME J. of Turbomachinery, 116, pp. 358-368.

[11] Walters, D. K., and Leylek, J. H., 1997, "A Detailed Analysis of Film- Cooling Physics Part I: Streamwise Injection with Cylindrical Holes", ASME J. of Turbomachinery, 122, pp. 102-112.

[12] Kusterer, K., Bohn, D., Sugimoto, T. and Tanaka, R., 2006, "Double-Jet Ejection of Cooling Air for Improved Film-cooling", ASME-paper GT2006-90854, Barcelona, Spain. (also published in 2007, ASME J. of Turbomachinery, 129, pp. 809-815).

[13] KHI and B&B-AGEMA: Japanese Patent JP2011196360.

[14] Lempereur, C., Andral, R. and Prudhomme, J. Y., "Surface temperature measurement on engine components by means of irreversible thermal coatings", Meas. Sci. and Technol. 19, 2008

[15] Taniguchi, T., Ryozo, T., Shinoda, Y., Ryu, M., Application of an Optical Pyrometer to Newly Developed Industrial Gas Turbine", ASME-paper GT2012-68679, Copenhagen, Denmark, 2012.

[16] Kusterer, K.,Lin, G., Moritz, N. and Bohn, D. "20 Years of of Experiences for the Conjugate Heat Transfer Analysis of Convection-cooled Turbine Vanes", ISJPPE-2012-B0076, Xi'an, China, 2012.

[17] Lemmon, E.W., Huber, M.L., McLinden, M.O., NIST Standard Reference Database 23: Reference Fluid Thermodynamic and Transport Properties-REFPROP, National Institute of Standards and Technology, Standard Reference Data Program

[18] VDI Gesellschaft, VDI Heat Atlas, 1988.

[19] Kusterer, K., Dickhoff, J., Sugimoto, T., Ryozo, T., Kazari, M., Custer, C., Dewan, Y., Schroeder, W., Bohn, D., "Improvement of the NEKOMIMI Film Cooling Technology by Application of an Automated Optimization Algorithm", IGTC, Tokyo, Japan, 2015.

[20] Kusterer, K., Tekin, N., Wüllner, T., Tanaka, R., Sugimoto, T., Kazari, M., Bohn, D. Bohn, D., "Nekomimi film cooling hole configurations under conjugate heat transfer condition", ASME-paper GT2014-25845, Duesseldorf, Germany, 2014.